

Effect of strain rate on the kinetics of hot deformation of AZ31 with different initial texture

M.Sanjari¹, A. Nabavi², S.A.Farzadfar¹, In-Ho Jung¹, S.Yue¹, E.Essadiqi³

¹Department of Materials Engineering, McGill University, Montreal, Canada

²Department of Mechanical Engineering, McGill University, Montreal, Canada

³CANMET – Materials Technology Laboratory, Ottawa, Canada

Keywords: Magnesium alloy, Texture evolution, Dynamic Recrystallization

Abstract

In this work, the effects of strain rate and initial texture on the flow behaviour and microstructure evolution on AZ31 Mg alloy were studied by compression tests. Cast plates were, homogenized and hot rolled and then compression tests were performed on samples with longitudinal axes either parallel to the rolling direction (RD) or the normal direction (ND). Compression tests were performed to various strains and samples were quenched to investigate the effect of dynamic recrystallization on the texture and microstructural evolution. Results show that for the samples machined in both rolling and normal direction, the rate of texture evolution is increased by increasing strain rate. The deformation mechanism was changed by increasing the strain rate for ND samples and at strain rate of 1 s⁻¹ from slip dominated flow to twin dominated flow. By using EBSD, the deformation mechanism and twinning types were investigated and double and tension twins were detected.

1. Introduction

Of all the industrially significant metals and alloys, magnesium alloys are known as lightweight high strength material and therefore are very attractive in applications such as automotive, railway and aerospace industries [1, 2]. One of the major obstacles for using magnesium alloys is their poor formability because of their hexagonal close-packed (hcp) crystal structure and therefore insufficient number of slip systems [3]. The main deformation mechanisms for Mg-alloys are slip and twinning. At room temperature the principal slip system is basal. At higher temperatures, several non-basal slip systems such as prismatic and pyramidal are activated due to temperature dependency of critical resolved shear stress of these slip systems [1, 4]. In the case of twinning, there are two commonly observed twin planes, {10 $\bar{1}$ 2} and {10 $\bar{1}$ 1} , that accommodate extension and contraction along the c-axis, respectively [5, 6]. These slip systems usually generate the basal texture during deformation with the basal poles aligning with the compression axis in compression test and the sheet normal direction during rolling [7, 8]. Current research is focused on generating a fine grained uniform microstructure and desirable (i.e. non-basal) texture using conventional production processes combined with alloying design. To optimize the parameters for hot deformation processing, it is mandatory to understand the effects of temperature and strain rate and also initial texture and microstructure on flow behaviour and microstructure evolution. The effect of initial texture on the plastic deformation of magnesium alloys at different temperature has been studied [9-11]. However, the effect of strain rate has rarely been examined systematically. Therefore the aim of this work is to study the effect of crystallographic texture and strain rate on the subsequent texture and microstructure development during hot deformation of AZ31. To do this, the kinetics of hot deformation are studied

using compression test on the samples were machined from as-cast and rolled samples in two normal and rolling direction.

2. Experimental procedure

This study was carried out on an AZ31B alloy with the following chemical composition (%wt): 3% Al, 0.9% Zn, 0.67% Mn and Mg (balance). The as-cast material was homogenized at 450 °C for 4 hr, which was found to give a consistent hot deformation behavior. This resulted in a coarse grain size of about 200 μ m measured by image analysis. To investigate the effect of strain rate on the microstructure and texture evolution, two series of tests were performed on the material in the temperature range from 300 °C to 450 °C. In order to apply low strain rates (0.01 and 1s⁻¹), a computer controlled servo-hydraulic materials testing system (MTS) with a 100 kN capacity was used. Specimens were deformed to strains of about 0.3 and 0.7 in order to observe the effect of strain on the microstructure. For higher strain rates, a cam plastometer was used, which is a reliable method for determining dynamic behavior at strain rates of the order of 10 to 100s⁻¹. Cylindrical samples, 9 mm in height and 6 mm in diameter, were used for lower compression tests. Because the anvil motion is fixed in the cam plastometer, in order to apply the strains of 0.3 and 0.7, two different sizes, 12 mm height with 9 mm diameter, and 21 mm height with 14 mm diameter were used. The deformed samples were sectioned through parallel to the longitudinal direction in order to examine microstructure and the texture. The samples were mounted and ground to 1200 grit and then polished with alcohol based 3 and 1 micron diamond suspensions for microstructural examination by optical microscopy. The samples were finally etched with an acetic-picric solution (10 mL acetic acid + 4.2 g picric acid + 10 mL water + 70 mL ethanol (99.5 pct)).

In texture analysis, a Siemens D-500 X-ray diffractometer equipped with a texture Goniometer using Co radiation was used. The samples for X-ray diffraction examination were prepared by grinding with SiC papers up to 1200 grit, and then polished with diamond suspension up to the grades of 3 and 1 micron. The data were analyzed to calculate orientation distribution function and to recalculate the pole figures.

3. Results and discussion

3.1 As-cast samples

3.1.1 Effect of strain rate on the flow behavior

Figure 1 shows typical flow curves at 375°C and at true strain rates of 0.01-100 s⁻¹. Generally, with increasing temperature or decreasing strain rate the flow curves are shifted to lower stress levels. In all curves, a peak stress was observed, although this was not as pronounced at 100 s⁻¹. The peak stress indicates a dynamic softening. After the peak, the stress decreases gradually, Figure 2 shows the effect of strain rate on the peak strain at constant temperatures. As can be seen, by increasing the strain rate the peak strain increases. This can be explained by the fact of time

and temperature dependency of dynamic recrystallization. At lower strain rate there is more time available to move boundaries and the higher temperature increases the rate of boundary motion [12].

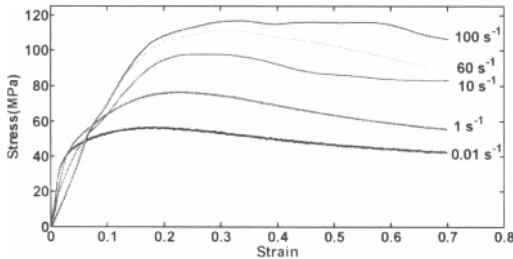


Fig. 1 The stress-strain curve at various strain rate and temperature of 375 °C.

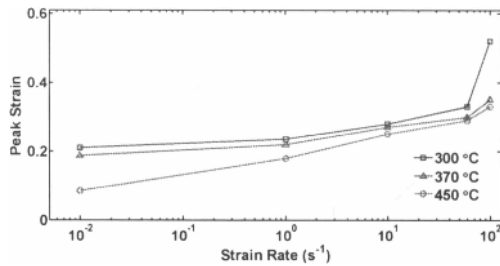


Fig. 2 The effect of strain rate on the peak strain of AZ31 at different temperature and strain rates

3.1.2 Microstructural characterization of as-cast material

The microstructural evolution was studied by examining the specimens obtained after deformation according to two criteria: (i) samples deformed up to a fixed strain but at different strain rates and temperatures, and (ii) specimens obtained after deformation at constant strain rate and temperatures at two different strains. Figure 5 shows optical micrographs of samples deformed at temperature 375 °C and strain rates of 0.01, 1, 10, 60 and 100 s⁻¹. At the lower strain rates of 0.01 and 1 s⁻¹ the necklace structure can be seen in the grain boundaries of initial grains. The mechanism of DRX in these deformation conditions has been analysed by McQueen and Knopieva [13]: Basal slip in favourably oriented grains takes place and twinning also occurs to reorient grains not suited for slip. When the strain reaches a sufficiently high level, DRX can occur at locations with high misorientations, which have been generated by accommodation of dislocations. Due to several slip systems activated near the grain boundary, there are more dislocations and therefore new fine grains form a necklace along grain boundaries. These regions appear to continually undergo recrystallization, possibly because deformation is easier compared to the grain core.

By increasing the strain rate, more twins were observed and this can be proved by the shifting of the shape of curves from convex to concave indicating that deformation mode changes from slip-dominated flow to twin-dominated flow [14]. The volume fraction of DRX grains is higher than at lower strain rates. There is limited time for the movement of dislocations at the high strain rate deformation, and therefore twins are formed to help deformation even at the higher temperatures [10]. In general, when twins exist in the deformed microstructure, DRX takes place at both grain

and twin boundaries. However, the influence of twin boundaries increases when the alloys are deformed at higher strain rates simply because the volume fraction of twins is increasing. Grosvenor et al [15] observed twinning induced DRX in cast AZ31. In AZ31 at 250°C and low strain rate, twinning induced DRX was not been observed; however, at 400°C and at high strain rate, twins can be a suitable place for DRX nucleation [16]. Three steps were suggested for twinning induced DRX: creation of the twinning boundary, transformation to a high angle boundary and migration of this boundary [16]. Yin et al [17] suggested that distortion energy accumulated by twinning and the activation of dislocations plays an important role for the nucleation of DRX. Note that because of the initial large grain size in the AZ31B used in this work, grain boundary sliding would be very difficult.

As Fig. 3e revealed, the recrystallization volume fraction rises with the increase of strain rate. Beer et al. [18] suggested that the kinetics of recrystallization is promoted with increasing the strain rate and decreasing the temperature due to higher stored energy at larger values of Z. Since this statement is valid for metadynamic recrystallization [18, 19], it may explain why there is increasing volume fraction of recrystallised microstructure at higher strain rates.

3.1.3 Texture evolution

Fig. 4 shows the (0002) pole figures of the samples deformed under different strain rates at a temperature of 375 °C and strain of 0.3. The deformation texture after compression is similar to the strong basal texture observed in common Mg alloys, i.e. the c-axis of in most of the grains aligns with the direction of compressive strain [20]. However, the results show that the rate of texture evolution is increased with strain rate and the maximum intensity is increased from 2.4 to 3.2 for the samples deformed at 0.01 and 100 s⁻¹, respectively.

3.2 Effect of initial texture on deformation behavior (rolled material)

3.2.1 Flow curves

Selected flow curves obtained during the hot deformation of the as-cast and rolled material in two directions are shown in figure. 4. As can be seen from this figure, in both strain rates the stress level is much higher for the as-cast material compared to either of the rolled samples. Comparing the rolled materials, the effect of initial texture on the flow stress is significant pre-peak strain, but is non-existent after the peak strain has been reached. The pre-peak differences are much more pronounced at the higher strain rate of 1s⁻¹.

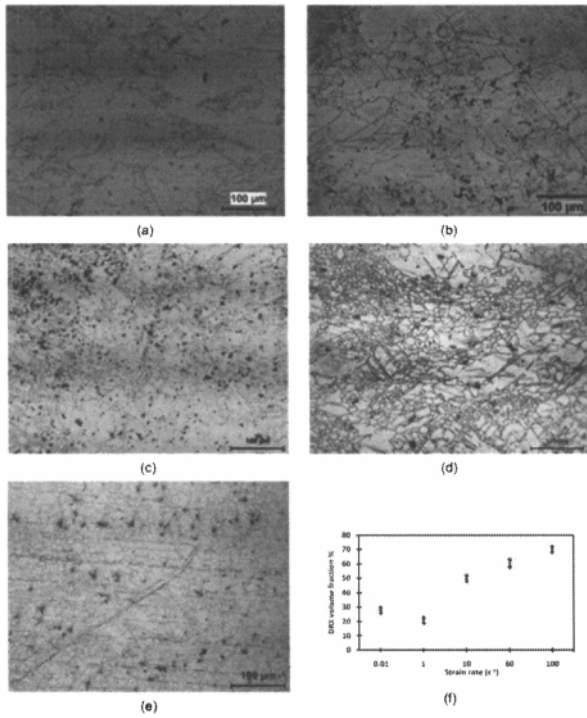


Fig. 3 Microstructures of the specimens compressed to the strain of 0.3 at 375 °C and strain rate of (a) 0.01 s⁻¹, (b) 1 s⁻¹, (c) 10 s⁻¹, (d) 60 s⁻¹, and (e) 100 s⁻¹ (f) DRX volume fraction at different strain rates

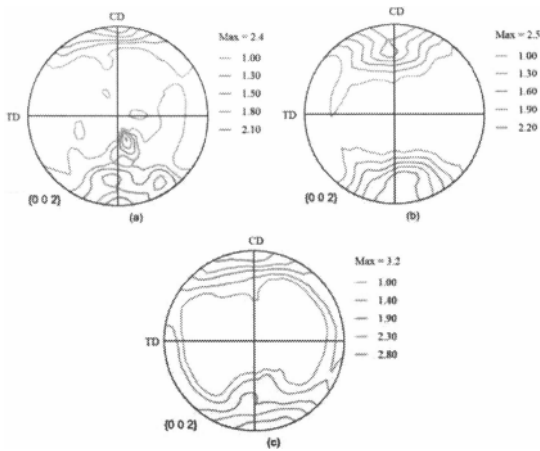


Fig. 4 [0002] X-ray pole figure of the specimens compressed to the strain of 0.3 at 375 °C and strain rates of (a) 0.01 s⁻¹, (b) 10 s⁻¹, and (c) 100 s⁻¹.

3.2.2 Slip systems

To find reasons for the above observations, the [0002] pole figure representing the texture of the samples before deformation for ND and RD samples was calculated from the ODF and shown in Fig. 6. As can be seen the basal poles are parallel and perpendicular to the compression axis for the ND and RD samples, respectively. Based on the initial configuration of the basal poles, the potential slip systems in the samples during compression test are discussed below.

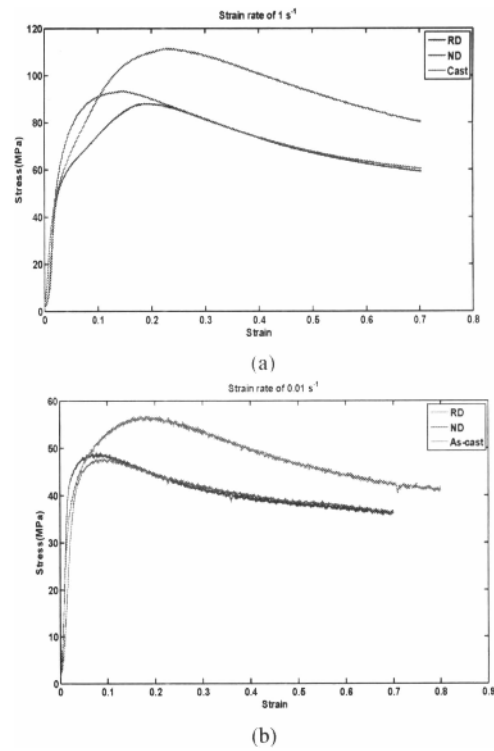


Fig. 5. The flow curves for the as-cast, RD and ND samples deformed at 375°C and strain rate of (a) 1 s⁻¹ and (b) 0.01 s⁻¹

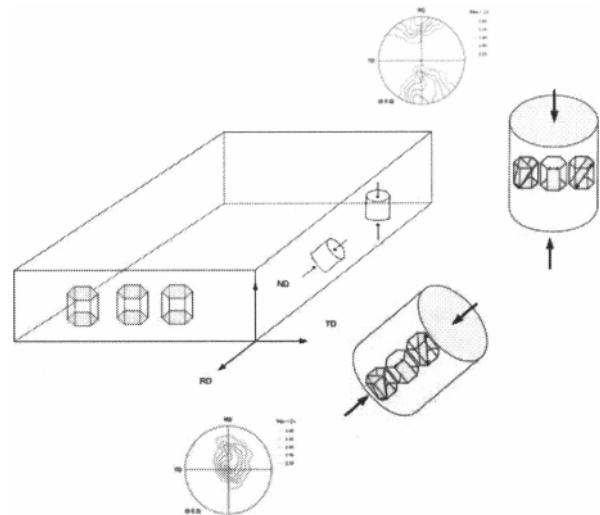


Fig. 6. Specimen orientation and their initial texture with respect to the rolled sheet geometry.

3.2.2.1 ND samples:

In this sample the basal planes are almost perpendicular to the compression axis and therefore basal slip is very much reduced. The prismatic slip system is also unfavourable since $\{10\bar{1}0\}$ planes are parallel to the compression axis. Although the first-order pyramidal planes are favourably oriented, the slip direction $\langle 11\bar{2}0 \rangle$ is almost normal to the direction of applied stress therefore their activation is difficult. In the case of second-order pyramidal, the slip direction is also favourable for slip; however, the relatively high value of the CRSS for this slip would prevent slip at room temperature, but at elevated temperature this system may be activated. In summary, in the ND samples the orientation of the basal planes is favourable for second-order pyramidal slip, and has all other slip systems having much smaller contributions to slip.

3.2.2.2 RD samples

In RD samples, as can be seen in figure 6, the $\{0002\}$ planes are oriented parallel to the compression axis and therefore the activity of the basal slip system reduces considerably. The prismatic planes can be oriented parallel, perpendicular or at about 30° respect to the compression axis. The latter orientation can be activated to a limit amount. If the basal planes are considered to be completely parallel to the compression axis, the first-order pyramidal slip planes, $\{10\bar{1}1\}$, will be oriented at about 28° or 46° with respect to the compression axis. The other first-order pyramidal plane, $\{11\bar{2}0\}$, is oriented at 46° or 60° respect to the compression axis which is favourable for slip. It is important to note that the slip direction $\langle 11\bar{2}0 \rangle$ can be oriented in 90° from the compression axis and therefore cannot contribute to the slip. The second-order pyramidal slip planes $\{11\bar{2}2\}$ can also be activated during the deformation. In summary, from the initial orientation point of view, for the samples compressed parallel to the rolling direction, basal slip is not a favourable slip system, limited prismatic slip can be activated if the grains have the appropriate direction. The first and second order pyramidal slip systems are highly favoured at the temperature (375°C) that deformation was performed and cross-slip can also occur on the pyramidal slip systems.

3.2.3 Twinning

As mentioned in the introduction, due to lower value of critical shear stress of the basal slip system, plastic deformation of Mg alloys appears to occur entirely by the basal slip modes at lower temperature. However basal slip provides only two independent slip systems. Therefore, it is expected that twinning, in particular $\{11\bar{1}2\}$ type, is increased by reducing the temperature. Lee et. al reported that increasing the strain rate has the same effect of reducing the temperature on increasing the number of twins [11]. The formation of $\{11\bar{1}2\}$ twins in magnesium lattices decreases the length of the crystal in a direction parallel to the basal plane and reorients the basal plane 86° into orientations which resist slip, with the c-axis more or less parallel to the loading axis. Therefore at least a part of rapid rise in the flow curves is due to twinning and an almost a linear part can be distinguished just prior to the peak. The twinning signature in the flow curves can also be investigated by plotting $d^2\sigma/d\varepsilon^2$ versus strain [5]. The present of a local maximum at strain lower than peak strain can be considered as sign of twinning in the deformed samples. As can be seen in Fig. 7 at temperature of 370°C by increasing the strain rate from 0.01 to 1 s^{-1} a local maximum can be detected in the curve. In the flow curve that exhibits the twinning signature, the strain to the peak flow stress is extended out to the higher value. By increasing the strain rate at constant temperature, more twins

were observed and this can be proved by the shifting shape of curves from convex to concave indicating that deformation mode changes from slip-dominated flow to twin-dominated flow [14]. As can be seen in Figure 8, twins can also be detected in the microstructure. It was reported that due to the preferential activation of twinning on the $\{10\bar{1}2\}$ $[\bar{1}011]$ in RD samples, this type of twinning plays a major role during the deformation [4]. Therefore, to study the deformation mechanism and twinning type more precisely, EBSD was performed to study the orientations of the twin and recrystallized areas. As can be seen in Fig. 7, at 375°C and a strain rate of 1 s^{-1} , twinning can easily be detected in the microstructure. From the misorientation angle distributions, the samples show local maxima in the range of $30\text{-}40^\circ$, $55\text{-}60^\circ$ and $85\text{-}90^\circ$. The maximum in the range of $30\text{-}40^\circ$ with a dominant $\langle -12\text{-}10 \rangle$ rotation axis can be attributed to the presence of $\{10\text{-}11\}$ - $\{10\text{-}12\}$ double twins. The second peak, $55\text{-}60^\circ$, is related to the clustering of rotation axes near $\langle 01\text{-}10 \rangle$. These misorientation relationships occur between twins that form on either the $(10\text{-}12)$ and $(01\text{-}12)$ planes. The last peak is attributed to the propagation of $\{1\text{-}210\}$ twinning [5, 21]. The most common misorientation angle at this temperature, $85\text{-}90^\circ$, indicates the presence of the extension twins. Twinning activity increases with increasing strain rates and decreasing temperature [21]. Therefore, more twins can be detected in samples deformed at strain rate of 1 s^{-1} . This is because individual twins frequently form with high effective interface velocities and they can apparently develop much more rapidly than a slip band [11]. Therefore, at higher strain rates, twinning plays a more important role due to less activity of slip. In ND samples, because most of the grains are oriented in a way that their c-axes are parallel to the compression axis, contraction twins can form and the basal planes are reoriented by 56° around $\langle 1021 \rangle$ axis. This change facilitates glide on the basal planes and generates zones of flow localization. These twins can undergo extension twinning in their interiors that is referred to double twinning.

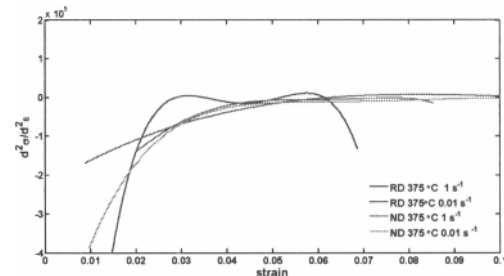


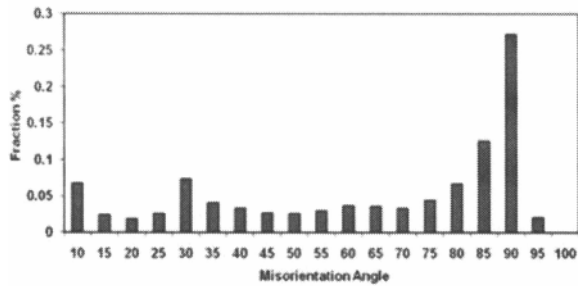
Fig. 7. A plot of change in the work hardening ($d^2\sigma/d\varepsilon^2$) against strain for RD and ND samples deformed at 375°C .

3.2.4 Texture evolution

Fig. 8 shows the (0002) pole figures of the RD samples deformed under different strain rates and strains. The initial basal pole distribution is perpendicular to the compression axis and as deformation is performed the basal poles tilt to the compression axis. The results show that the rate of texture evolution is increased by increasing strain rate. At a strain of 1 s^{-1} a basal pole



(a)



(b)

Fig. 7. (a) Orientation map and (b) misorientation angle distribution of the samples deformed at strain rate of 10 s^{-1} and temperature of $375 \text{ }^\circ\text{C}$ and strain of 0.1.

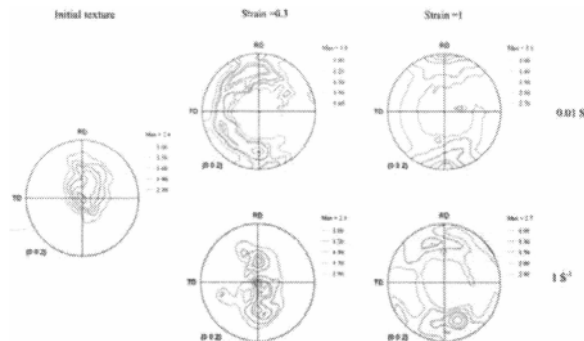


Fig 8. Texture evolution for RD samples deformed at strain rate of 1 s^{-1} and different strains and temperature of $375 \text{ }^\circ\text{C}$

figure typical for compression testing was achieved after strain of 1; however, for strain rate of 0.01 s^{-1} the pole figure still affected by the initial texture. As mentioned in the previous section by increasing the strain rate, the fraction of extension twinning increases in the deformed RD samples and basal planes are reoriented by 86° around a $\langle 1021 \rangle$ axis; therefore the basal texture forms. It was observed that the recrystallization of Mg alloys is not accompanied with an obvious change of crystallographic texture [12]. Because of a higher level boundary energy grain boundaries and twins can both be the nucleation sites for DRX. DRX on twins is more important than the DRX on grain boundaries for the microstructure evolution during higher strain rate deformation because there are more twins. On the other hand,

the c-axis of the twin DRX grain is parallel to the compression stress. Such a grain orientation cannot deform easily and is not favorable for basal slip because the resolved shear stress is nearly zero. Therefore, these grains are less hardened compared with the grains with other orientations and relatively stable and insensitive to DRX. However, new grains with other orientations may easily be consumed by repeated DRX. With deformation progress, more and more grains with their c-axes parallel to compression stress would survive. Therefore, the basal texture is progressively strengthened.

Conclusion

The hot compression flow stress and microstructure evolution of AZ31b alloys at different strain rates and different initial texture were investigated. The following conclusions can be drawn from the analysis:

- (1) At higher strain rates ($\geq 10 \text{ s}^{-1}$), twins form, and since DRX occurs at twins, this explains why DRX is more extensive at higher strain rates. This also results in a more homogeneous microstructure compare.
- (2) The EBSD results show that the type of twins activated in RD samples are double twins and extension twinning.
- (3) Correlations of the orientation of slip systems and the axis of compression revealed that the hot deformation of the RD specimens involves activation of first- and second-order pyramidal slip while that of ND specimens occurs by second order pyramidal slip.
- (4) The results show that the rate of texture evolution in RD samples is increased by increasing strain rate because of increasing the fraction of extension twinning.

Acknowledge

The authors would like to thank Prof. In-Ho Jung for his kind support. Thanks are also due to the Natural Resources Canada's CANMET materials technology laboratory for careful technical support. This study was supported by the NSERC Magnesium Strategic Research Network (MagNET) and MEDA Fellowship from Faculty of Engineering of McGill University.

- [1] H.B. M. Avedesian, ASM specialty handbook. Magnesium and magnesium alloys. , ASM International, Materials Park, Ohio, 2000.
- [2] T. Mukai, Materials Science and Technology, 16 (2000) 1314-1319.
- [3] S.R. Agnew, M.H. Yoo, C.N. Tomé, Acta Materialia, 49 (2001) 4277-4289.
- [4] S. Spigarelli, M.E. Mehtedi, M. Cabibbo, E. Evangelista, J. Kaneko, A. Jäger, V. Gartnerova, Materials Science and Engineering: A, 462 (2007) 197-201.
- [5] M.R. Barnett, Materials Science and Engineering: A, 464 (2007) 1-7.
- [6] J.W. Christian, S. Mahajan, Progress in Materials Science, 39 (1995) 1-157.
- [7] Q. Guo, H.G. Yan, H. Zhang, Z.H. Chen, Z.F. Wang, Materials Science and Technology, 21 (2005) 1349-1354.
- [8] Q. Jin, S.-Y. Shim, S.-G. Lim, Scripta Materialia, 55 (2006) 843-846.
- [9] M.T.S. E. Essadiqi, A. Javaid, C. Galvani, K. Spencer, S. Yue, and R. Verna, in: International Conference on Light Metals Technology, Saint-Sauveur, Quebec, Canada, 2007, pp. 177-182.

- [10] K. Ishikawa, H. Watanabe, T. Mukai, *Materials Letters*, 59 (2005) 1511-1515.
- [11] B.H. Lee, W. Bang, S. Ahn, C.S. Lee, *Metallurgical and Materials Transactions A: Physical Metallurgy and Materials Science*, 39 A (2008) 1426-1434.
- [12] A.G. Beer, M.R. Barnett, *Materials Science and Engineering: A*, 423 (2006) 292-299.
- [13] H.J. McQueen, E.V. Konopleva, in, 2001, pp. 227-234.
- [14] M.R. Barnett, Z. Keshavarz, A.G. Beer, D. Atwell, *Acta Materialia*, 52 (2004) 5093-5103.
- [15] A. Grosvenor, C.H.J. Davies, in, 2003, pp. 4567-4572.
- [16] S.E. Ion, F.J. Humphreys, S.H. White, *Acta Metallurgica*, 30 (1982) 1909-1919.
- [17] D.L. Yin, J.T. Wang, J.Q. Liu, X. Zhao, *Journal of Alloys and Compounds*, 478 (2009) 789-795.
- [18] A.G. Beer, M.R. Barnett, *Materials Science and Engineering A*, 485 (2008) 318-324.
- [19] A. Mwembela, E.B. Konopleva, H.J. McQueen, *Scripta Materialia*, 37 (1997) 1789-1795.
- [20] T. Al-Samman, G. Gottstein, *Materials Science and Engineering A*, 490 (2008) 411-420.
- [21] K. Ishikawa, H. Watanabe, T. Mukai, *Journal of Materials Science*, 40 (2005) 1577-1582.